



2- μm Brillouin laser based on infrared nonlinear glass fibers

M. DEROH,^{1,2,*} B. KIBLER,² A. LEMIERE,² F. DESEVEDAVY,² F. SMEKTALA,² H. MAILLOTTE,¹ T. SYLVESTRE,¹ AND J.-C. BEUGNOT¹ 

¹Institut FEMTO-ST, UMR 6174 CNRS, Université Bourgogne Franche-Comté, Besançon, France

²Laboratoire Interdisciplinaire Carnot de Bourgogne, UMR 6303 CNRS, Université Bourgogne Franche-Comté, Dijon, France

*Corresponding author: moise.deroh@femto-st.fr

Received 7 May 2019; revised 4 July 2019; accepted 11 July 2019; posted 12 July 2019 (Doc. ID 367025); published 7 August 2019

Infrared fiber materials such as chalcogenide, tellurite, and heavily germanium-doped silica glasses are attractive materials for many applications based on nonlinear optical effects such as Kerr, Raman, and Brillouin processes. Here, we experimentally demonstrate a close-to-single-frequency Brillouin fiber laser in the 2- μm wavelength region either based on tellurite (TeO_2) glass or on heavily germanium-doped silica glass. Our results reveal a strong enhancement of the Brillouin gain efficiency at 2 μm of more than 50 times that of standard silica optical fibers. A lasing threshold and narrow linewidth of 98 mW and 48 kHz, respectively, have been demonstrated in the tellurite fiber-based laser. This simple Brillouin laser source configuration confirms the potential applications of such fibers for the development of nonlinear photonic devices in the important 2- μm spectral range. © 2019

Optical Society of America

<https://doi.org/10.1364/AO.58.006365>

1. INTRODUCTION

Stimulated Brillouin scattering (SBS) in optical fibers is a key nonlinear optical effect with important applications such as distributed optical fiber sensing, microwave photonics, Brillouin spectroscopy, optical storage and fiber lasers [1–5]. The latter application has attracted significant interest as highly coherent laser sources with sub-hertz (Hz) linewidth have recently been achieved using SBS in simple all-fiber passive optical cavities and in high-Q resonators [6–8]. To date, most Brillouin lasers have been designed to operate at telecom wavelengths ($\sim 1.55 \mu\text{m}$) based on several materials such as a silica-on-silicon disk resonators [9], highly nonlinear fibers (HNLF) [10], tellurite-based optical fibers [11], and chalcogenide glass photonic chips and fibers [12,13]. However, for a range of mid-infrared applications like high-resolution molecular sensing and coherent LIDAR, there is a need to develop narrow-linewidth laser sources at longer wavelengths. Recently, only a few studies on Brillouin fiber lasers (BFLs) have been reported in the 2- μm spectral range [14–16]. For instance, Luo *et al.* demonstrated in 2014 a single-frequency BFL operating at 2 μm , in which three strong pump diodes with a total power of 18 W were employed to overcome a high lasing threshold of 1.04 W [14]. The lasing threshold was later lowered to 52 mW using a chalcogenide ($\text{As}_{38}\text{Se}_{62}$) glass suspended-core optical fiber as the Brillouin gain medium [15]. In another study, a widely tunable Brillouin laser based on a thulium-doped fiber laser pump and a segment of highly germanium-doped silica optical fiber (75 mol% GeO_2

doping level) has been demonstrated with a low threshold of 47 mW only [16].

Tellurite (TeO_2) glasses also appear as very attractive materials for Brillouin scattering around 2 μm . In addition to providing high Brillouin gain efficiency and narrow linewidth, they also exhibit low loss beyond 2 μm compared to silica glass [14]. To the best of our knowledge, no 2- μm BFLs based on a tellurite optical fiber or heavily GeO_2 -doped-core silica optical fiber with 98 mol% doping level have been reported yet.

In this paper, we demonstrate a low-threshold single-frequency BFL at 2 μm based on step-index tellurite (TeO_2) optical fiber. Our results reveal very good performances at 2 μm compared to previous works. More specifically, a lasing threshold and narrow linewidth of 98 mW and 48 kHz, respectively, have been demonstrated, which thus confirm the strong potential of soft-glass fibers for Brillouin applications. We further investigated the potential of a heavily GeO_2 -doped-core silica optical fiber with a 98 mol% doping level for Brillouin lasing at 2 μm , and we show a higher power threshold up to 645 mW.

The paper is organized as follows: We first investigate SBS in a short segment of each fiber to get the Brillouin frequency shift and threshold. A Brillouin laser cavity is then experimentally investigated by using a passive fiber ring cavity configuration incorporating the TeO_2 -based optical fiber. Finally, we compare and discuss the performances of the BFL developed at 2 μm with another heavily GeO_2 -doped-core silica optical fiber and with previous works using a chalcogenide-glass ($\text{As}_{38}\text{Se}_{62}$) optical fiber and a standard single-mode silica fiber (SMF-28).

2. EXPERIMENTAL SETUP

Figure 1 shows a simple configuration of the BFL similar to that described in Ref. [13]. A tunable narrow-linewidth continuous-wave diode laser around $2\ \mu\text{m}$ (Thorlabs TLK-L1950R) was used as a pump laser. The pump wave was amplified up to 29.5 dBm using a thulium-doped fiber amplifier (TDFA) and injected into the nonlinear fiber under test (FUT) by use of an optical circulator (OC). An additional short segment of ultrahigh-numerical-aperture (UHNA) fiber was used for butt coupling into TeO_2 glass-based fibers. A 99:1 fiber tap coupler was inserted to extract and characterize the BFL signal, while the remaining 99% of the Stokes wave was fed back into the passive fiber ring cavity. The Brillouin Stokes wave, in this configuration, perform multiple round-trips, while the pump laser that travels in the backward direction is isolated by the circulator. A polarization controller was also inserted into the cavity to ensure that the polarization of the Stokes wave is kept parallel to that of the pump laser to maximize the Brillouin gain. The output BFL light is then sent into an optical spectrum analyzer (OSA, Yokogawa AQ6375) with a resolution of 10 GHz and a high-speed $2\text{-}\mu\text{m}$ photodiode (PD, Newport, 818-BB-51AF) for optical and radio-frequency (RF) spectrum measurements.

The fiber cavity consisted of a 2-m-long segment of tellurite step-index fiber whose core and cladding compositions are $80\text{TeO}_2\text{-}5\text{ZnO-}10\text{Na}_2\text{O-}5\text{ZnF}_2$ (TZNF, molar fraction) and $60\text{TeO}_2\text{-}5\text{ZnO-}20\text{Na}_2\text{O-}15\text{GeO}_2$ (TZNG), respectively. Another 1.8-m-long segment of heavily GeO_2 -doped-core optical fiber with a 98 mol% doping level was used for a further comparison. The optical circulator, polarization controller, and fiber coupler are all made of standard single-mode silica fiber (SMF1950) with a total length of 3 m that belongs to the cavity (i.e., the total cavity length is equal to 5 or 4.8 m, respectively). The corresponding free spectral range (FSR) of both cavities under study is estimated in the ~ 40 MHz range, close to the Brillouin gain linewidth, so the number of longitudinal modes that can be amplified under the Brillouin gain spectrum is approaching unity. Here, we note that our $4\text{-}\mu\text{m}$ core diameter tellurite fiber is not strictly single mode around $2\ \mu\text{m}$ and that it has linear losses of about $0.5\ \text{dB}\cdot\text{m}^{-1}$, a low anomalous dispersion regime, and a high nonlinear Kerr coefficient of

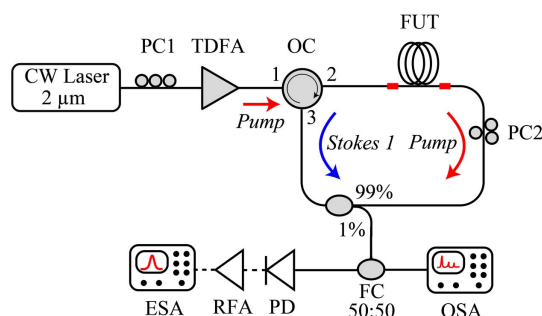


Fig. 1. Experimental setup of Brillouin fiber laser cavity. CW, continuous wave; TDFA, thulium-doped fiber amplifier; PC, polarization controller; OC, optical circulator; FC, fiber coupler; FUT, fiber under test; OSA, optical spectrum analyzer; RFA, radio-frequency amplifier; ESA, electrical spectrum analyzer; PD, photodiode.

about $0.12\ \text{W}^{-1}\cdot\text{m}^{-1}$ (for details, see Ref. [17]). With the tellurite fiber, the total cavity losses were measured to be around 9.5 dB due to 2.5 dB butt-coupling loss at each fiber facet and 3.5 dB loss related to other fiber components. Regarding the heavily GeO_2 -doped-core silica fiber with a $2\text{-}\mu\text{m}$ core diameter, it exhibits single-mode behavior at $2\ \mu\text{m}$ and anomalous group-velocity dispersion; the linear losses are $0.1\ \text{dB}\cdot\text{m}^{-1}$, and its nonlinear coefficient is found to be about $0.03\ \text{W}^{-1}\cdot\text{m}^{-1}$ (more details can be found in Ref. [18]). The GeO_2 -doped-core silica fiber was directly spliced to other standard fiber components of the cavity (with splice loss per facet about 1 dB), so the total cavity losses were measured to be around 5.7 dB.

3. RESULTS WITH TELLURITE FIBER

The Brillouin frequency shift (BFS, ν_B) and its linewidth were experimentally measured at $2\ \mu\text{m}$ in the spontaneous regime (almost 17 dB below the Brillouin critical threshold) by using a standard heterodyne detection technique like that described in Ref. [19].

Figure 2 shows the experimental Brillouin spectrum of the TeO_2 -based fiber for an input power of 15 dBm. The SBS gain spectrum exhibits a main frequency peak at 6.165 GHz (BFS) and a secondary weak peak down to 6.15 GHz. By fitting the Brillouin gain spectrum with a Lorentzian function (red dashed curve), we can estimate the Brillouin linewidth ($\Delta\nu_B$) as 14.9 MHz, which is lower than that measured at $1.55\ \mu\text{m}$ (about 21 MHz) for $\nu_B = 7.972\ \text{GHz}$, and the latter values at $1.55\ \mu\text{m}$ are close to those previously reported in Ref. [20]. Tuning the pump wavelength around $2\ \mu\text{m}$ indeed slightly changes the SBS frequency and linewidth because of the phase-matching condition that depends on the optical wavelength, as $\nu_B = 2n_{\text{eff}}V_a/\lambda_p$, where n_{eff} , V_a , and λ_p are effective index, longitudinal acoustic velocity, and optical wavelength, respectively. All these opto-acoustic parameters of the TeO_2 -based fiber are listed in Table 1 together with other tested fibers (GeO_2 , $\text{As}_{38}\text{Se}_{62}$, and SMF-28). The SBS gain coefficient can be straightforwardly estimated from the Brillouin gain linewidth using the equation in Ref. [19], and this gives $g_B = 1.05 \times 10^{-10}\ \text{m}\cdot\text{W}^{-1}$. The theoretical single-pass Brillouin threshold (P_{th}) is 1.87 W (32.7 dBm) based on the following equation [1]:

$$P_{\text{th}} = \frac{21 \times A_{\text{eff}} \times K}{g_B \times L_{\text{eff}}}, \quad (1)$$

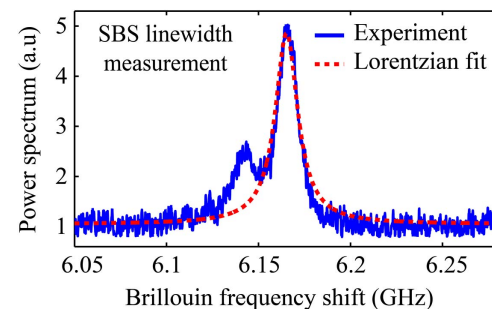


Fig. 2. Experimental Brillouin spectrum of the step-index tellurite-glass optical fiber.

Table 1. Optoacoustic and Brillouin Lasing Parameters of Tellurite, Germanium (GeO₂), Chalcogenide (As₃₈Se₆₂), and Standard Silica Optical Fibers (SMF-28)

Optical Fiber	TeO ₂ ^a	GeO ₂ ^a	As ₃₈ Se ₆₂ ^b	SMF-28 ^c
Core size, Φ (μm)	4	2	4.5	8.2
Loss, α (dB · m ⁻¹)	0.5	0.1	2.2	0.022
Length, L (m)	2	1.8	1.5	14
Eff. length, L _{eff} (m)	1.6	1.76	1.13	13.5
Eff. area, A _{eff} (μm ²)	10	5	8	101
Ref. index, n	1.968	1.580	2.81	1.45
Eff. index, n _{eff}	1.944	1.514	-	1.443
Acoustic velocity, V _a (m · s ⁻¹)	3155	3898	2173	5960
Mass density, ρ (kg · m ⁻³)	6000	3596	4640	2210
Figure of merit, FOM (γ * Leff * Pth)	0.376	0.495	0.283	0.089
SBS frequency, ν _B (GHz)	6.165	6.00	6.258	8.38
SBS linewidth, Δν _B (MHz)	14.9	76	21.5	15
SBS gain coef. g _B (×10 ⁻¹¹ m · W ⁻¹)	10.5	1.02	350	2.87
SBS efficiency, g _B /A _{eff} (m ⁻¹ · W ⁻¹)	10.5	2.04	437.5	0.28
SBS threshold, P _{th} (W)	1.871	8.764	0.0914	8.203
BFL threshold, P _{th,S1} (mW)	98	645	52	1040
BFL linewidth, Δν _{BFL} (kHz)	48	1500	4000	8

^aValues from this work.

^bValues from Ref. [15].

^cValues from Refs. [14,23].

where A_{eff}, g_B, and L_{eff} are the effective fundamental mode area, the Brillouin gain coefficient, and the effective length, respectively, and K = 1.5.

Figure 3(a) depicts the Brillouin laser spectra close to 2 μm for an increasing coupled power into the tellurite fiber from 56.2 to 223 mW (from 17.5 to 23.5 dBm). Note that the

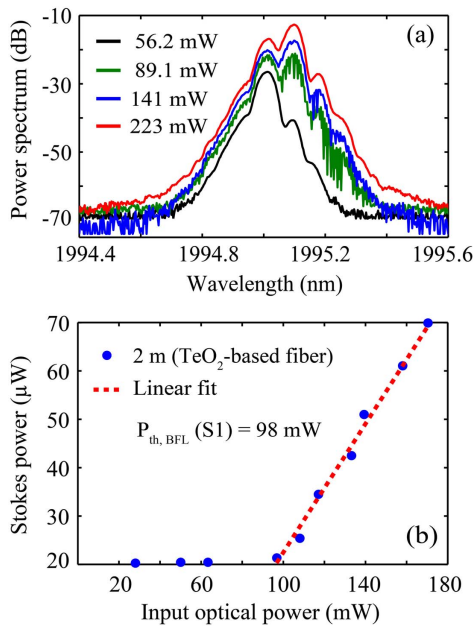


Fig. 3. (a) Experimental BFL optical spectra obtained with the TeO₂-based fiber by varying input pump power; (b) Stokes wave power versus input optical power (Port 1).

pump power is measured from port 1 of the OC. We clearly see that Brillouin lasing occurs from 89.1 mW (green spectrum) as an upper wavelength shift of 82 pm that matches the SBS frequency and thus confirms that the Brillouin gain is strong enough to compensate for the ring cavity losses beyond the threshold. For higher input powers, the first Stokes wave grows significantly and then generates a second-order Stokes wave and so on. We still note the presence of the backward pump at 1995 nm due to strong Fresnel reflections (about 10%) at the tellurite fiber end facet. In Fig. 3(b), we show the Stokes power as a function of the input pump power. The backscattering weak power level (20 μW) recorded at low pump power comes from the both Fresnel losses and Rayleigh scattering. The TeO₂-based BFL exhibits a low threshold of 98 mW for this single-pass pumping configuration. Similar experiments using 1.5 m of chalcogenide fiber (As₃₈Se₆₂) and 140 m of standard silica fiber (SMF-28) have been reported in Refs. [14,15]. A close lasing power threshold was obtained with the chalcogenide fiber, whereas for the SMF-28 fiber it is almost 5 times larger due to poor light confinement and strong absorption at 2 μm.

We further investigated the coherence properties of our BFLs in the electrical domain using the heterodyne detection. Figure 4 shows the recorded RF beat signal between the Brillouin laser and the reflected optical pump light. The spectrum is centered at the BFS (6.156 GHz), and the full width at half-maximum (FWHM) of the BFL is estimated to be 48 kHz using a Lorentzian fit, which thus shows a significant linewidth narrowing compared to the spontaneous regime (14.9 MHz, Fig. 2). We must stress, however, that this is just a measurement of the beat signal, which is slightly greater than the laser linewidth. The delayed self-heterodyne technique [21] would be preferable to precisely measure the BFL linewidth. However, we note that this technique is difficult to implement at 2 μm due to the higher linear losses in long-delay silica fibers at 2 μm (around 22.2 dB/km) as described in Refs. [14,16]. However, the BFL linewidth can be estimated based on the input laser linewidth (~100 kHz) and the ring cavity parameters by using the following equations [22]:

$$\Delta\nu_{\text{BFL}} = \frac{\Delta\nu_{\text{pump}}}{D^2}, \quad (2)$$

$$D = 1 + \frac{\pi \times \Delta\nu_B}{-\frac{c}{nL} \times \ln R}, \quad (3)$$

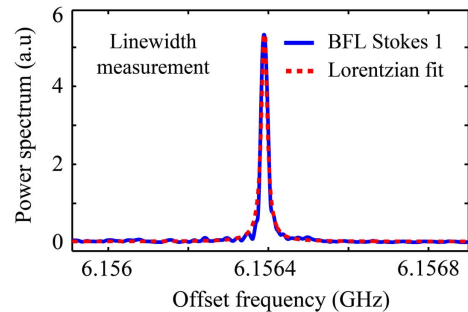


Fig. 4. Electrical spectrum of the TeO₂-based Brillouin fiber laser spectrum of the TeO₂-based optical fiber measured for an injected optical power of 112 mW (Port 1). RBW = 5 kHz, resolution bandwidth of the electrical spectrum analyzer (ESA).

where $\Delta\nu_{\text{BFL}}$, $\Delta\nu_{\text{pump}}$, c , n , L , and R are the linewidths of the Stokes wave and the optical pump, the speed of the light, the refractive index, the fiber length, and the cavity feedback parameter, respectively. The D factor is here estimated to be 1.51. The Brillouin fiber laser linewidth could be calculated to be 41 kHz, which is close to the experimental value.

4. RESULTS WITH HEAVILY GERMANIUM-DOPED-CORE SILICA FIBER

Both frequency and linewidth of the Brillouin gain spectrum at 2 μm (in the spontaneous regime, i.e., well below the Brillouin threshold) are again experimentally measured using the heterodyne detection in the case of a heavily GeO_2 -doped-core silica optical fiber. In such optical fibers, it has recently been demonstrated that the Brillouin gain (decibels, dB) greatly increases with the doping level [18]. Figure 5 shows the experimental backscattering Brillouin spectrum of this fiber when injected optical power is fixed to 25 dBm (Port 2). The SBS gain spectrum exhibits a single-frequency peak centered around 6 GHz (BFS, ν_B). As expected, this value is lower than the BFS at 1.55 μm pump wavelength, found to be 7.7 GHz in Ref. [18]. The Brillouin gain spectrum is fitted with a Lorentzian spectral profile (red dashed curve), and we obtain a Brillouin linewidth ($\Delta\nu_B$) of 76 MHz, which is almost 5 times larger than that of the TeO_2 -based fiber. The germanium doping here strongly contributes to the acoustic properties of the optical fiber, particularly broadening the SBS linewidth when compared to standard silica fibers [18] (see also Table 1). The SBS gain efficiency is then estimated to be $2.04 \text{ m}^{-1} \cdot \text{W}^{-1}$, which is almost 10 times larger than standard silica fibers ($0.28 \text{ m}^{-1} \cdot \text{W}^{-1}$). The theoretical Brillouin threshold (P_{th}) of the fiber without cavity feedback can be calculated to be 8764 mW (39.4 dBm). The SBS threshold is here very high due to the short length (1.8 m) used in our experiment.

Figure 6(a) shows the recorded optical Brillouin laser spectra at 2 μm using the GeO_2 -doped silica fiber-based cavity, when coupled optical power is increased from 27 to 29.5 dBm (501 to 891 mW). We note that the Brillouin lasing effect occurs around 28.5 dBm (orange spectrum). Beyond the laser threshold, we again retrieve a cascade of Stokes waves.

The reflected laser pump can be observed on the short wavelength side centered at 1988.35 nm due to the Fresnel reflection estimated to be around 5%. In Fig. 6(b), we show the Stokes wave power as a function of the input pump power

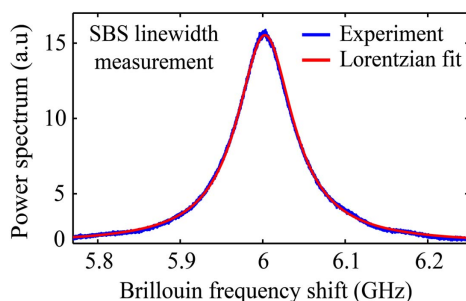


Fig. 5. Experimental Brillouin spectrum of the 98-mol% GeO_2 -doped-core silica fiber obtained for an injected optical power of 25 dBm (Port 2).

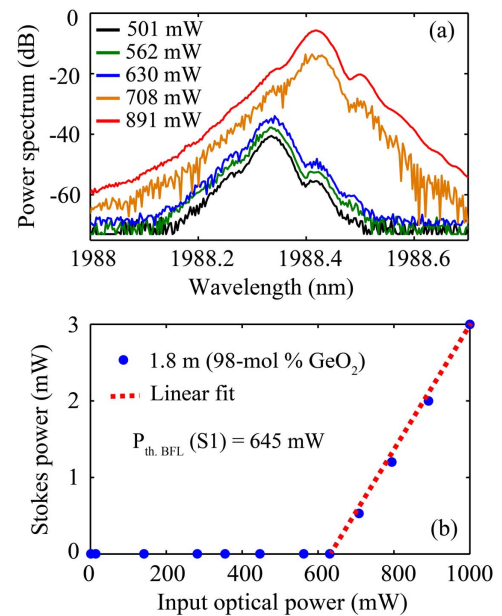


Fig. 6. (a) Experimental Brillouin laser spectra of the heavily GeO_2 -doped-core silica optical fiber with an increased input pump power; (b) extracted Stokes wave power versus injected optical power (Port 1).

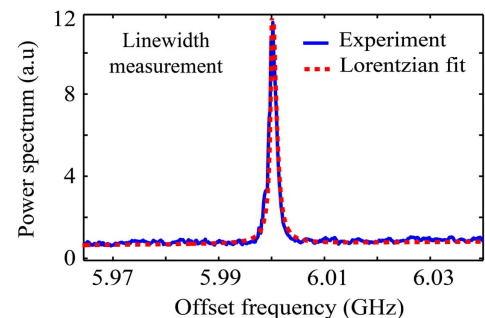


Fig. 7. Electrical spectrum of the heavily- GeO_2 -doped Brillouin fiber laser spectrum of the heavily GeO_2 -doped-core silica optical fiber (98-mol %) at 707 mW as injected optical power.

(Port 1). The GeO_2 -doped-core silica fiber exhibits a lasing threshold of 645 mW for this single-pass pumping configuration, which is very high compared to the TeO_2 -based fiber.

Figure 7 depicts the RF beat signal between the Brillouin laser and the reflected optical pump light when the input power is 707 mW (Port 1). The resulting RF spectrum is centered at the Brillouin frequency of 6 GHz, and the FWHM of the BFL laser is estimated to be 1.5 MHz, which is very large compared to the expected value (5.2 kHz) calculated with Eqs. (2) and (3).

5. DISCUSSION AND CONCLUSION

Our results showed that the advantage gained by using the tellurite glass fiber is in fact twofold. First, regarding the intrinsic property of the material, the TeO_2 -based fiber, in a similar way to chalcogenide-glass fiber, exhibits a very narrow Brillouin

linewidth. Second, based on the high SBS efficiency of the tellurite fiber, the characteristics of the Brillouin laser (low threshold, narrow linewidth) are already comparable to the best configurations. Table 1 summarizes all the experimental and theoretical results of this paper and shows the comparison of both optical and acoustic properties between optical fiber samples used in this work and other recent studies at 2- μm wavelength. Both effective index (n_{eff}) of the fundamental optical mode and effective area (A_{eff}) were numerically calculated using a finite-element method (COMSOL software) and including opto-geometric parameters of the fibers. We also provided the figure of merit (FOM) as defined in Ref. [24]. From Table 1, we can underline the strong Brillouin gain efficiency of the tellurite fiber in the 2 μm band, about 52 times larger than that of an SMF-28, as well as the low laser threshold. It is worth noting that the SBS gain efficiency of the $\text{As}_{38}\text{Se}_{62}$ optical fiber remains very high compared to all fiber materials presented in the table. For all fibers, BFL linewidth measurements are listed, but the delayed self-heterodyne technique cannot be used due to the high linear losses at 2 μm when kilometer (km)-long delay fibers are required. Another technique would be preferable in this wavelength region.

To conclude, a close-to-single-frequency Brillouin fiber laser has been demonstrated at 2- μm wavelength using a short length (≤ 2 m) of either step-index tellurite fiber or heavily GeO_2 -doped-core silica fiber. The backscattering SBS characterization reported shows a strong enhancement of the Brillouin gain efficiency compared to standard silica fibers at 2 μm . A BFL threshold of 98 and 645 mW have been obtained in the passive ring cavity, while the BFL linewidth is found to be 48 kHz and 1.5 MHz. Improvement of the cavity losses is under study in the particular case of tellurite fiber to advantageously increase the laser efficiency. This simple configuration of BFL laser is proposed as a promising candidate for developing narrow-linewidth laser sources in the 2- μm band and beyond for molecular gas sensing, spectroscopy, and infrared applications.

Funding. Agence Nationale de la Recherche (ANR) (ANR-17-EUR-0002, ANR-15-IDEX-0003, ANR-16-CE24-0010-03); Conseil Régional de Bourgogne-Franche-Comté.

REFERENCES

1. G. P. Agrawal, *Nonlinear Fiber Optics* (Academic, 2007).
2. C. A. Galindez-Jamióy and J. M. Lopez-Higuera, "Brillouin distributed fiber sensors: an overview and applications," *J. Sens.* **2012**, 204121 (2012).
3. A. Godet, A. Ndao, T. Sylvestre, V. Pecheur, S. Lebrun, G. Pauliat, J.-C. Beugnot, and K. P. Huy, "Brillouin spectroscopy of optical microfibers and nanofibers," *Optica* **4**, 1232–1238 (2017).
4. M. Merklein, B. Stiller, K. Vu, S. J. Madden, and B. J. Eggleton, "A chip-integrated coherent photonic-phononic memory," *Nat. Commun.* **8**, 574 (2017).
5. K. O. Hill, B. S. Kawasaki, and D. C. Johnson, "cw Brillouin laser," *Appl. Phys. Lett.* **28**, 608–609 (1976).
6. M. C. Colloido, F. Sedlmeir, B. Sprenger, S. Svitlov, L. J. Wang, and H. G. L. Schwefel, "Sub-kHz lasing of a CaF_2 whispering gallery mode

- resonator stabilized fiber ring laser," *Opt. Express* **22**, 19277–19283 (2014).
7. S. Huang, T. Zhu, G. Yin, T. Lan, L. Huang, F. Li, Y. Bai, D. Qu, X. Huang, and F. Qiu, "Tens of hertz narrow-linewidth laser based on stimulated Brillouin and Rayleigh scattering," *Opt. Lett.* **42**, 5286–5289 (2017).
8. W. Loh, A. A. S. Green, F. N. Baynes, D. C. Cole, F. J. Quinlan, H. Lee, K. J. Vahala, S. B. Papp, and S. A. Diddams, "Dual-microcavity narrow-linewidth Brillouin laser," *Optica* **2**, 225–232 (2015).
9. J. Li, H. Lee, and K. J. Vahala, "Microwave synthesizer using an on-chip Brillouin oscillator," *Nat. Commun.* **4**, 2097 (2013).
10. M. I. Kayes and M. Rochette, "Optical frequency comb generation with ultra-narrow spectral lines," *Opt. Lett.* **42**, 2718–2721 (2017).
11. G. Qin, H. Sotobayashi, M. Tsuchiya, A. Mori, T. Suzuki, and Y. Ohishi, "Stimulated Brillouin scattering in a single-mode tellurite fiber for amplification, lasing, and slow light generation," *J. Lightwave Technol.* **26**, 492–498 (2008).
12. I. V. Kabakova, R. Pant, D.-Y. Choi, S. Debbarma, B. Luther-Davies, S. J. Madden, and B. J. Eggleton, "Narrow linewidth Brillouin laser based on chalcogenide photonic chip," *Opt. Lett.* **38**, 3208–3211 (2013).
13. K. H. Tow, Y. Léguillon, S. Fresnel, P. Besnard, L. Brilland, D. Méchin, D. Trégoat, J. Troles, and P. Toupin, "Linewidth-narrowing and intensity noise reduction of the 2nd order Stokes component of a low threshold Brillouin laser made of $\text{Ge}_{10}\text{As}_{22}\text{Se}_{68}$ chalcogenide fiber," *Opt. Express* **20**, B104–B109 (2012).
14. Y. Luo, Y. Tang, J. Yang, Y. Wang, S. Wang, K. Tao, L. Zhan, and J. Xu, "High signal-to-noise ratio, single-frequency 2 μm Brillouin fiber laser," *Opt. Lett.* **39**, 2626–2628 (2014).
15. K. Hu, I. V. Kabakova, T. F. S. Büttner, S. Lefrancois, D. D. Hudson, S. He, and B. J. Eggleton, "Low-threshold Brillouin laser at 2 μm based on suspended-core chalcogenide fiber," *Opt. Lett.* **39**, 4651–4654 (2014).
16. T. Yin, B.-M. Mao, Y. Wei, and D. Chen, "Widely wavelength-tunable 2 μm Brillouin fiber laser incorporating a highly germania-doped fiber," *Appl. Opt.* **57**, 6831–6834 (2018).
17. C. Strutyński, P. Froidevaux, F. Désévéday, J.-C. Jules, G. Gadret, A. Bendahmane, K. Tarnowski, B. Kibler, and F. Smektala, "Tailoring supercontinuum generation beyond 2 μm in step-index tellurite fibers," *Opt. Lett.* **42**, 247–250 (2017).
18. M. Deroh, B. Kibler, H. Maillotte, T. Sylvestre, and J.-C. Beugnot, "Large Brillouin gain in germania-doped core optical fibers up to a 98 mol% doping level," *Opt. Lett.* **43**, 4005–4008 (2018).
19. J.-C. Beugnot, T. Sylvestre, D. Alasia, H. Maillotte, V. Laude, A. Monteville, L. Provino, N. Traynor, S. F. Mafang, and L. Thévenaz, "Complete experimental characterization of stimulated Brillouin scattering in photonic crystal fiber," *Opt. Express* **15**, 15517–15522 (2007).
20. K. S. Abedin, "Stimulated Brillouin scattering in single-mode tellurite glass fiber," *Opt. Express* **14**, 11766–11772 (2006).
21. L. Richter, H. Mandelberg, M. Kruger, and P. McGrath, "Linewidth subcoherence delay times," *IEEE J. Quantum Electron.* **22**, 2070–2074 (1986).
22. A. Debut, S. Randoux, and J. Zemmouri, "Linewidth narrowing in Brillouin lasers: theoretical analysis," *Phys. Rev. A* **62**, 023803 (2000).
23. A. Sincore, N. Bodnar, J. Bradford, A. Abdulfattah, L. Shah, and M. C. Richardson, "SBS threshold dependence on pulse duration in a 2053 nm single-mode fiber amplifier," *J. Lightwave Technol.* **35**, 4000–4003 (2017).
24. J. H. Lee, T. Tanemura, K. Kikuchi, T. Nagashima, T. Hasegawa, S. Ohara, and N. Sugimoto, "Experimental comparison of a Kerr nonlinearity figure of merit including the stimulated Brillouin scattering threshold for state-of-the-art nonlinear optical fibers," *Opt. Lett.* **30**, 1698–1700 (2005).